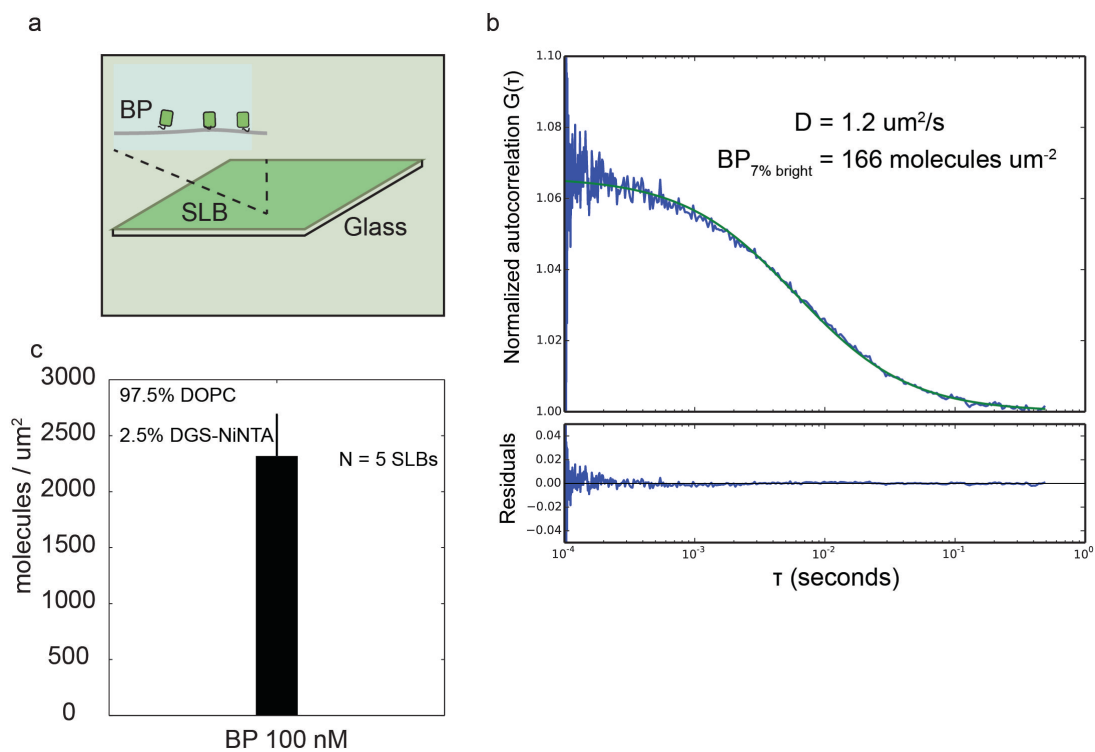


## Supplementary Information to the manuscript

### Size-dependent protein segregation at membrane interfaces

Eva M Schmid<sup>1\*</sup>, Matthew Bakalar<sup>\*2</sup>, Kaushik Choudhuri<sup>3</sup>, Julian Weichsel<sup>4,5</sup>,  
HyoungSook Ann<sup>1,6</sup>, Phillip L Geissler<sup>2,4,8</sup>, Michael L Dustin<sup>3,8</sup>, Daniel A Fletcher<sup>1,2,8,†</sup>

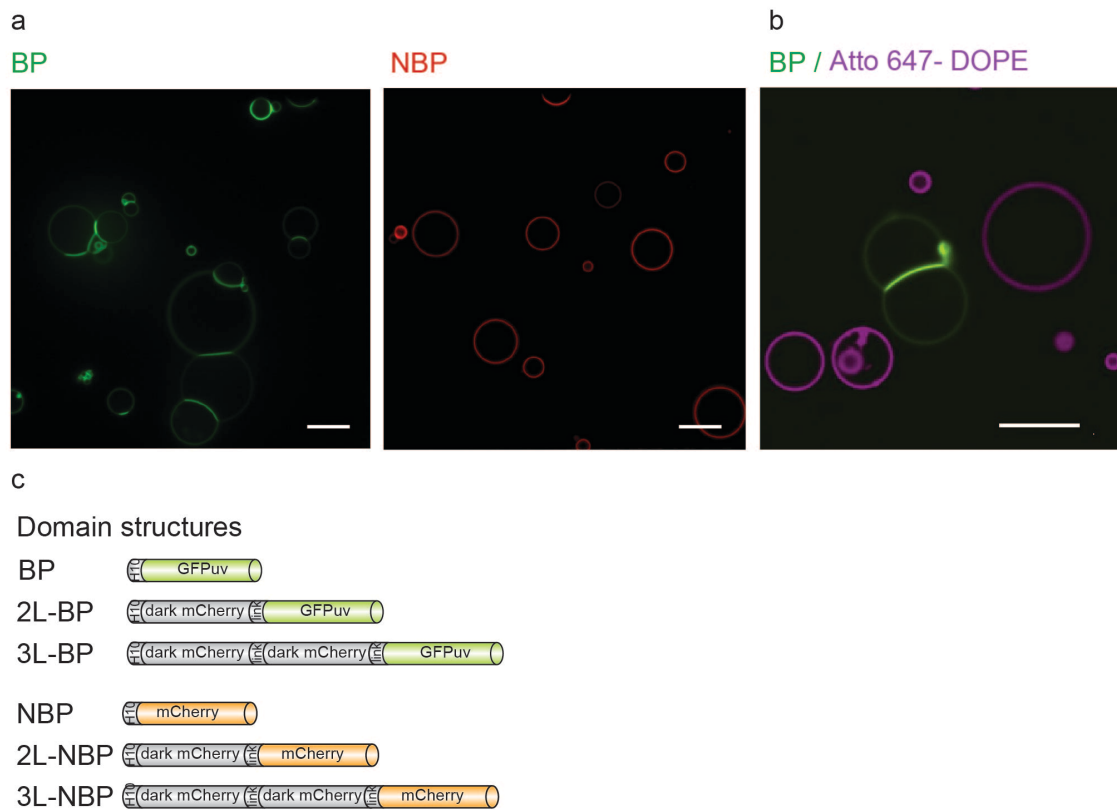
### Supplementary Figure S1. BP density measurement by FCS



**(a)** Glass supported lipid bilayers (SLBs, composition: 94.47% DOPC, 2.5% DOGS-NiNTA) are incubated 100 nM BP solution for 10 minutes. **(b)** The density of BP protein on the SLB is measured by FCS. 7% fluorescent GFPuv (BP) was mixed with 93% mutated non-fluorescent GFPuv (BP-Y66S) (7% bright) is used to achieve the correct concentration range for FCS measurements. Normalized autocorrelation curves are fit with a single component two-dimensional diffusion model to extract the diffusion

coefficient and protein density of the BP (molecules/ $\mu\text{m}^2$ ) **(c)** Measurements on 5 independent SLBs reveal an BP density of 2,317  $\pm$  370 molecules/ $\mu\text{m}^2$  for an SLB with 2.5% DOGS-Ni-NTA incubated with 100 nM BP protein.

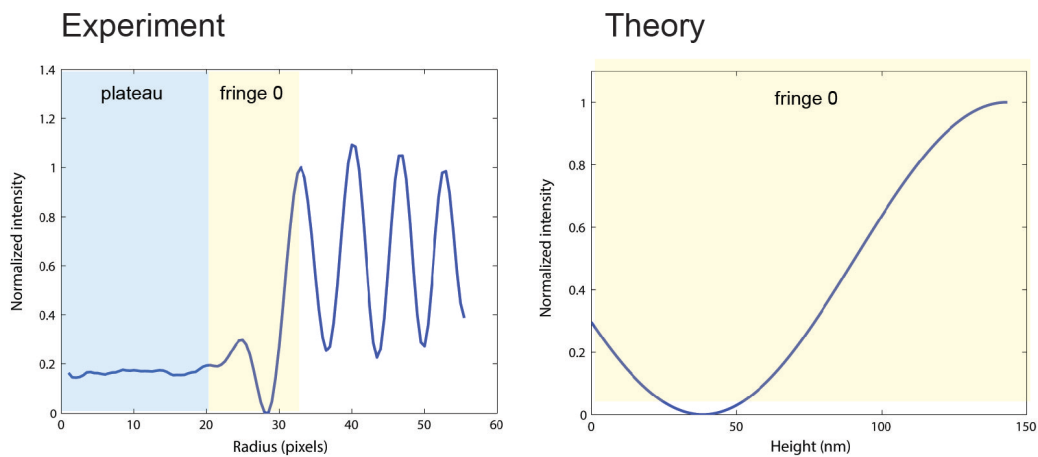
**Supplementary Figure S2.**



**(a)** Representative field of view of BP (green) and NBP (red) bound to DOGS-Ni-NTA containing GUV membranes (composition: 97.47% DOPC, 2.5% DOGS-Ni-NTA incubated with 100 nM protein solution for 10 min). Note how BP molecules form GUV interfaces while NBP molecules do not. Scale bar is 20  $\mu\text{m}$  long. **(b)** A mixture of GUVs with His-tagged protein binding capability (97.5% DOPC, 2.5% DOGS-Ni-NTA) and GUVs lacking DOGS-Ni-NTA (99.7% DOPC, 0.3% Atto647-DOPE) were incubated with 100 nM GFPuv (BP). BP only bound to DOGS-Ni-NTA containing vesicles, confirming

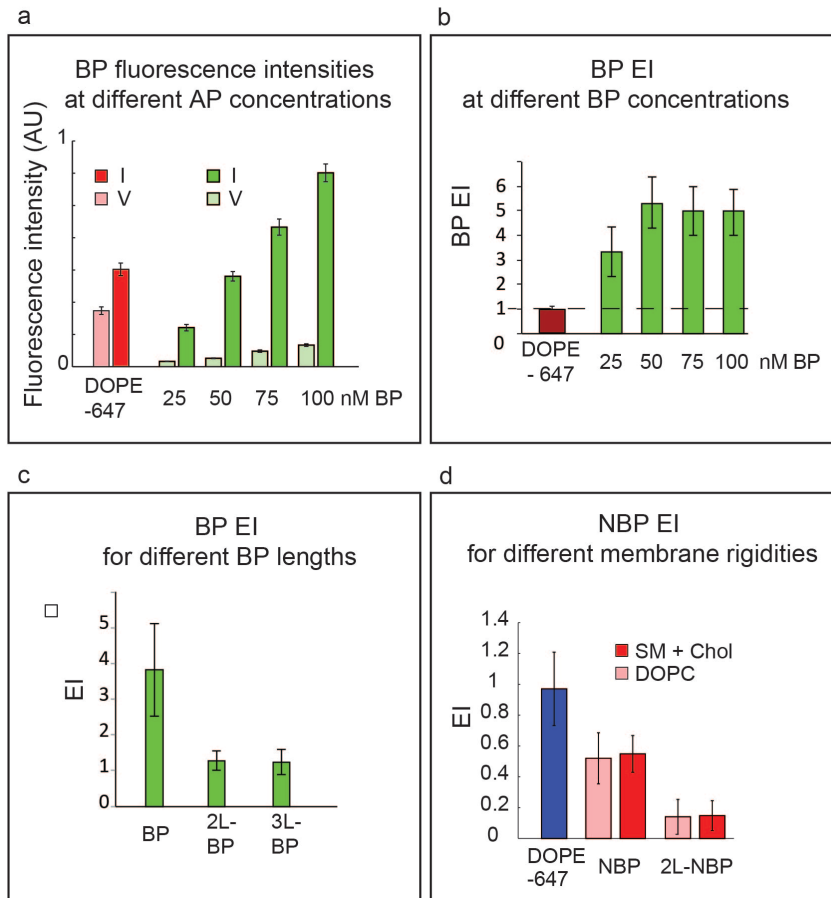
that there is no non-specific binding of BP from solution to membranes. Furthermore, we could not detect unspecific interface formation between BP-covered GUVs and protein-free GUVs. All scale bars are 10  $\mu\text{m}$ . **(c)** Protein domain architectures illustrate proteins used in this study.

### Supplementary Figure S3. Distance measurements by RICM



**(left)** Radially averaged RICM contrast as a function of the distance from the center of the GUV. **(right)** Theoretical RICM contrast as a function of the height of the variable buffer layer, which corresponds to the distance between SLB and the bottom surface of the GUV (see Methods).

## Supplementary Figure S4.



**(a)** Increasing concentrations of BP in solution leads to increased fluorescence intensities on GUVs. Vesicle (V) fluorescence intensities are plotted versus interface (I) intensities. **(b)** EIs for BP at different protein concentrations in solution. We note that while the intensities in a) scale with concentration, protein distribution over the vesicles stays remarkably constant at different protein densities. **(c)** EI values for different lengths adhesion molecules averaged over all experiments. Single lengths BP enrich more at the interface possibly due to higher 2D affinity than the longer 2L-BP and 3L-BP. **(d)** Exclusion of NBP or 2L-NBP from BP interfaces does not change significantly with increased membrane rigidity. GUVs from 80% Sphingomyelin and 20% Cholesterol mixtures (SM + Chol) have a approximately 6 fold higher bending rigidity than the DOPC

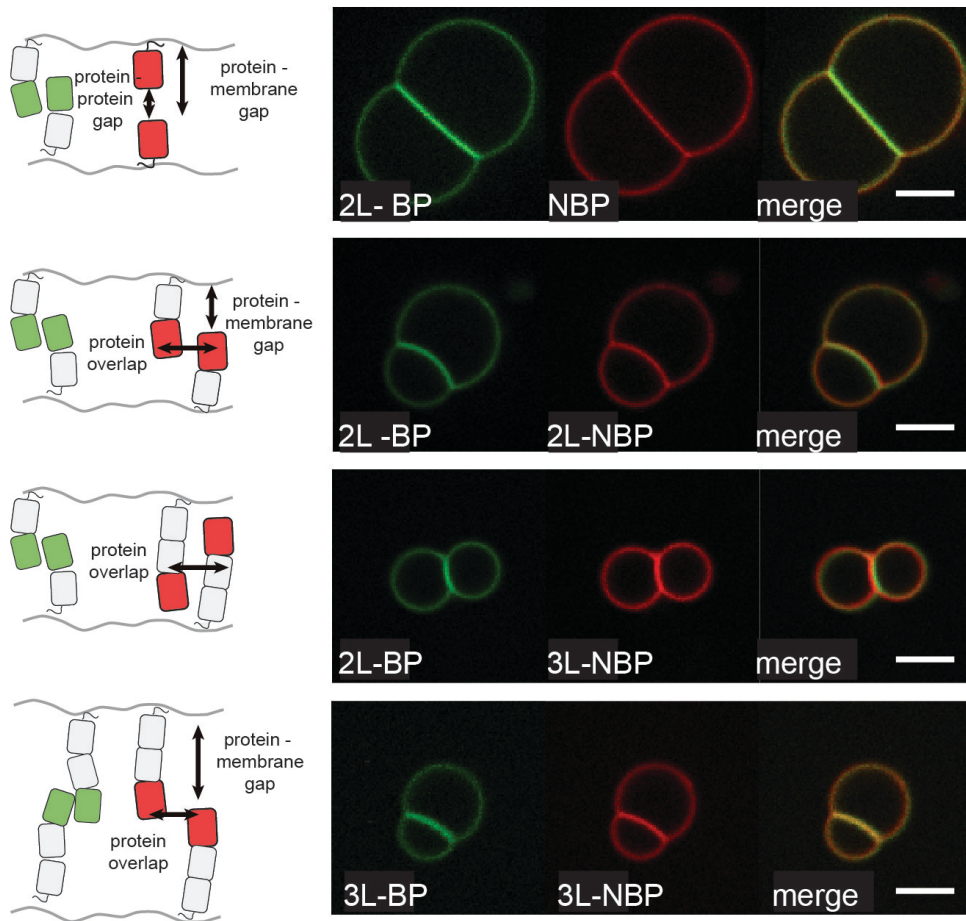
GUVs. SM+Chol (77.5% Brain Sphingomyelin (Avanti), 20% Cholesterol (Avanti) 2.5 % DOGS Ni-NTA) GUVs were incubated with 100 nM BP and 100 nM NBP or 2L-NBP. Interface formation and NBP and 2L NBP exclusion did not differ significantly from the same experiment performed on DOPC (97.5 % DOPC, 2.5% DOGS-NiNTA) vesicles.

### Supplementary Table. BP densities

	molecules per $\mu\text{m}^2$		% coverage per $\mu\text{m}^2$	
	V	I	V	I
100 nM BP in presence of NBP (100 nM)	2317*	11585	3.71	18.50
75 nM BP in presence of NBP (100 nM)	1674	8372	2.60	13.40
50 nM BP in presence of NBP (100 nM)	911	4830	1.50	7.70
25 nM BP in presence of NBP (100 nM)	580	1930	0.93	3.00
100 nM BP in presence of 2L-NBP (100 nM)	2317	8222	3.71	13.20
100 nM BP in presence of 3L-NBP (100 nM)	2317	6789	3.71	10.90
100 nM 2L-BP in presence of NBP (100 nM)	2317	3081	3.71	4.93
100 nM 2L-BP in presence of 2L-NBP (100 nM)	2317	2943	3.71	4.71
100 nM 2L-BP in presence of 3L-NBP (100 nM)	2317	2965	3.71	3.52
100 nM 3L-BP in presence of 3L-NBP (100 nM)	2317	2873	3.71	3.41

Summary of all estimated BP density values in molecules per  $\mu\text{m}^2$  and percent coverage per  $\mu\text{m}^2$ . \* density value was measured by FCS. All other density values were estimated by correlating fluorescence intensity values with measured density. Coverage was calculated using an estimated footprint of GFPuv of  $4 \text{ nm}^2$  (see Methods for details).

## Supplementary Figure S5



Representative confocal images for data in Fig. 4a. Increasing the size of the adhesive protein (2L-BP, 3L-BP) leads to decreased exclusion of NBP variants from interfaces. Representative confocal fluorescence images of GUVs (composition: 97.47% DOPC, 2.5% DOGS-Ni-NTA) incubated with 100 nM BP variants and 100 nM NBP variants in solution for 10 min. Scale bars are 5  $\mu\text{m}$  long (green channel: BP, red channel: NBP). Error bars are standard error of the mean from three independent experiments on separate vesicle batches, each with  $\sim 50$  vesicles categorized.